

Degradation of dye effluent*

J. P. Lorimer[‡], T. J. Mason, M. Plattes, S. S. Phull, and D. J. Walton

School of Science and Environment, Coventry University, Coventry CV1 5FB, UK

Abstract: Solutions of both basic and acidic dyes were subject to sonolysis, electrolysis, and sonoelectrolysis. Only basic dyes were decolorized by ultrasound alone. Removal of the acidic dye Sandolan Yellow required the use of an electrooxidation process. The rate of electrochemical decolorization in the absence of ultrasound was dependent on the type of electrolyte, the electrolyte concentration, the reaction temperature, and the current density. The sonoelectrooxidation of Sandolan Yellow needed to be performed in a sealed cell to minimize the effects of ultrasonic degassing.

INTRODUCTION

Two of the major dye groups are the “basic dyes” (e.g., Yoracyl Brilliant Red, Astrazon Red GTLN, Maxilon Blue GRL, Maxilon Blue 5G, Astrazon Golden Yellow GL, and Astrazon Green M) and the “acidic dyes” (e.g., Sandolan Yellow) (see Fig. 1).

Astrazon Red GTLN, Maxilon Blue GRL, and Sandolan Yellow belong to the group of dyes called azo dyes. They form the largest group of all the synthetic colorants and play a prominent part in almost every type of application. The chromophoric system consists essentially of the azo group, $-N=N-$ (Fig. 1), in association with one or more aromatic systems. For example, a consideration of the structure of Sandolan Yellow shows it contains further chromophores (conjugation) and auxochromes ($-OH$, $-SO_3$, $-Cl$). As more conjugated double bonds are added to a molecule, the energy required to reach the first excited state decreases. Auxochromes intensify the color of the dye and improve the substantivity of the dye for the substrate (fiber, yarn, etc.). Sandolan Yellow contains one azo group and therefore is called a monoazo dye.

Currently in the United Kingdom there are no requirements for color removal from dye effluent. The legislation varies from county to county and even depends on the actual conditions (river, sea, company, etc). One specific example of colored discharge requirements is given in Table 1 [1]. (Before measurement, the effluent is filtered through 0.45 μm filter paper and analyzed by UV–vis spectrophotometry using a 1-cm cell.)

Table 1 Example of absorbance limits.

Wavelength/nm	400	450	500	550	700
Absorbance	0.115	0.085	0.065	0.055	0.013

An example of the scale of the effluent problem for a typical textile spinning mill can be recognized when we consider that the daily dyeing process requirements are 2 tonnes of dye for 25 tonnes of

*An issue of reviews and research papers based on presentations made at the IUPAC/ICSU Workshop on Electrochemistry and Interfacial Chemistry in Environmental Clean-up and Green Chemical Processes, Coimbra, Portugal, 6–7 April, 2001.

[‡]Corresponding author

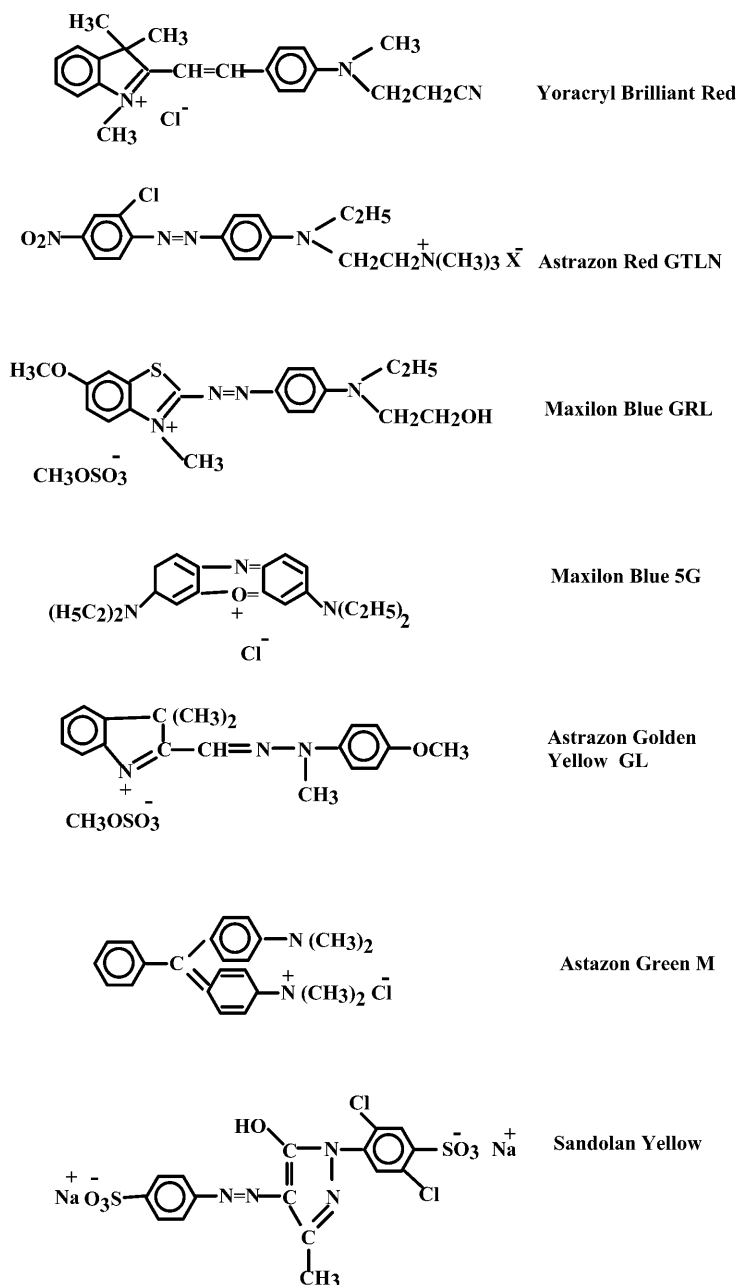


Fig. 1 Dye structures.

fiber; effluent volume is of the order of 850 m^3 with a dye concentration of 1.5 g dm^{-3} , which must be reduced to 1.5 mg dm^{-3} before discharge.

The traditional techniques for color removal are the use of activated carbon, filtration, coagulation, and treatment with ozone. Each method has advantages and disadvantages. For example, the use of charcoal is technically easy but has a high waste disposal cost. While filtration potentially provides

for the production of pure water, low-molar-mass dyes can pass through the filter system. Coagulation, using alums, ferric salts, or limes is also a low-cost process. However, it suffers from the disposal of the waste. Lastly, ozone, while not requiring a disposal procedure, suffers from high cost.

There is a large number of advanced oxidation processes currently being evaluated which use ultraviolet radiation (UV) in combination with hydrogen peroxide or titanium dioxide [2–5], ultrasound, or ultrasound in combination with ozonation [6–11] or electrochemistry [12–14].

The subject of this paper is the use of ultrasound, electrochemistry, and the simultaneous combination of the two techniques in the degradation of dye effluent.

EXPERIMENTAL

All dye materials were used as supplied and without further purification. Each dye was dissolved in water to provide an initial absorbance of approximately 1.2 au. For example, aqueous solutions of Astrazon Green ($\lambda_{\text{max}} = 617$ nm), Maxilon Blue GRL ($\lambda_{\text{max}} = 608$ nm), Maxilon Blue 5G ($\lambda_{\text{max}} = 654$ nm), and Yoracyl Brilliant Red ($\lambda_{\text{max}} = 512$ nm) were prepared to give initial concentrations of 15 mg dm^{-3} ; Astrazon Red GTLN ($\lambda_{\text{max}} = 487$ nm) solutions were prepared to give initial concentrations of 30 mg dm^{-3} ; Sandolan Yellow ($\lambda_{\text{max}} = 404$ nm) was prepared to provide an initial concentration of 50 mg dm^{-3} .

The effect of low-power, high-frequency ultrasound (1.1 W cm^{-2} , 510 kHz Undatim bath) on the degradation of several basics was investigated. The effect of both low-power, high-frequency ultrasound (1.1 W cm^{-2} , 510 kHz bath) and high-power, low-frequency ($20\text{--}100 \text{ W cm}^{-2}$; 20 kHz Sonics and Materials probe system; 6 and 29 W, 40 kHz bath, Langford Electronics) on the degradation of the acidic dye, Sandolan Yellow, was investigated. The response of the basic dye Astrazon Green M to different intensities of high-frequency (510 kHz) ultrasound was also studied.

The electrooxidation of various dyes in the presence and absence of ultrasound (510 kHz; 20kHz) was investigated as a function of electrolyte type, electrolyte concentration, current density, ultrasonic intensity, and reaction temperature. Electrolysis of several of the dyes was performed galvanostatically with either carbon or platinum electrodes both in the absence and presence of ultrasound. The carbon electrodes had a diameter of 6 mm and were immersed 7 cm into the solution, i.e., the electrode surface = 13.47 cm^2 . Each Pt-electrode had a surface area of 2 cm^2 . Samples were withdrawn at appropriate intervals, and the absorbance was measured by UV spectroscopy.

RESULTS AND DISCUSSION

Use of ultrasound alone

Figure 2 shows the effect of low-power (1.1 W cm^{-2}) high-frequency ultrasound (510 kHz) on three different basic dyes—Yoracyl Brilliant Red, Astrazon Golden Yellow GL, and Astrazon Red GTLN. It can be seen that the rate of disappearance of color is different in each case with Astrazon Red decolorizing the fastest and Yoracyl Brilliant Red decolorizing the slowest. In general, dyes with C=C bonds were easier to degrade.

Figure 3 shows the effect of different intensities (1.13, 0.76, and 0.27 W cm^{-2}) on the decolorization of Astrazon Green M. The figure shows that with increasing intensity there is an increase in the observed decolorization rate. The data can be fitted to a first-order decay to yield apparent “rate constant” whose values are 0.0054 min^{-1} ($I = 0.27 \text{ W cm}^{-2}$), 0.017 min^{-1} ($I = 0.76 \text{ W cm}^{-2}$) and 0.047 min^{-1} at the highest intensity (1.13 W cm^{-2}).

The acidic dye Sandolan Yellow was unaffected by ultrasound alone and raised the question whether it was in fact attacked by hydrogen peroxide (H_2O_2) or whether the concentrations produced on cavitation collapse were too low. Subsequent investigation revealed it was the former since there was no decolorization of the dye (50 mg dm^{-3}) even in the presence of 0.5 mol dm^{-3} peroxide.

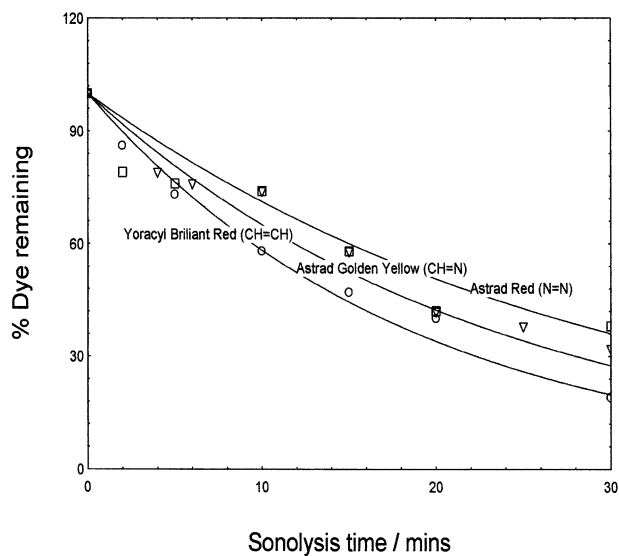


Fig. 2 High-frequency sonolysis at 510 kHz of Yoracyl Brilliant Red, Astrazon Golden Yellow GL, and Astrazon Red GTLN.

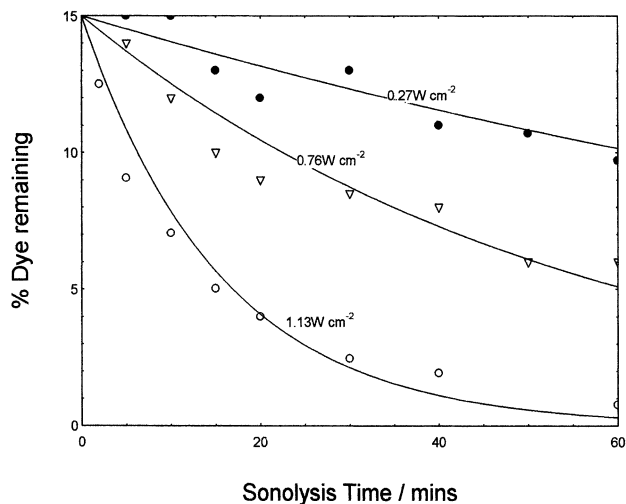


Fig. 3 Effect of intensity on the degradation of Astrazon Green M at 510 kHz.

However, the addition of hypochlorite solution ($2.5 \times 10^{-4} \text{ mol dm}^{-3}$) was effectively able to totally decolorize (97%) a solution ($1 \times 10^{-4} \text{ mol dm}^{-3}$) of Sandolan Yellow (Table 2).

Since one way of producing hypochlorite is to electrolyze an alkali metal chloride, electrolysis was used to produce hypochlorite *in situ* (eqs. 1–3)

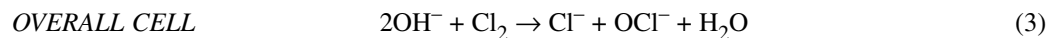
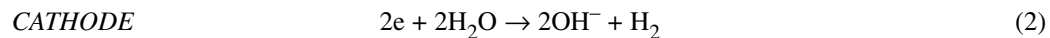
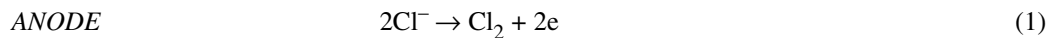


Table 2 Effect of hypochlorite concentration on Sandolan Yellow solutions ($9.07 \times 10^{-5} \text{ mol dm}^{-3}$).

Number	$[\text{OCl}^-]/(\text{mol dm}^{-3})$	Decolorization/% ^a
1	0.62×10^{-4}	49
2	1.24×10^{-4}	84
3	2.48×10^{-4}	97
4	3.72×10^{-4}	97
5	4.98×10^{-4}	97

^aThe percentage decolorization was calculated using the following equation:

$$\% \text{ Decolorization} = \frac{([\text{Abs}]_0 - [\text{Abs}]_t)}{[\text{Abs}]_0} \cdot 100. \text{ Here } [\text{Abs}]_0 = 1.16.$$

Electrooxidation in an open cell

As expected, hypochlorite was produced during the electrolysis of aqueous sodium chloride (0.5 mol dm^{-3}) as evidenced by the appearance of the OCl^- absorbance peak at 292 nm. In keeping with Faraday's law, the amount of hypochlorite produce was linear with time and therefore to the number of coulombs passed into the system (Fig. 4).

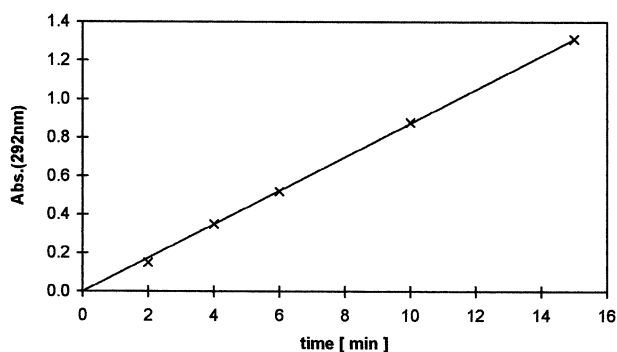


Fig. 4 Electrolysis of NaCl solution: (Pt-electrodes, $[\text{NaCl}] = 0.5 \text{ mol dm}^{-3}$, $V = 100 \text{ cm}^3$).

Effect of electrode material

Figure 5 shows the results of the electrolysis of an aqueous solution of Sandolan Yellow (50 mg dm^{-3}) using sodium chloride as electrolyte (0.2 mol dm^{-3}) and at a current of 100 mA at both carbon and

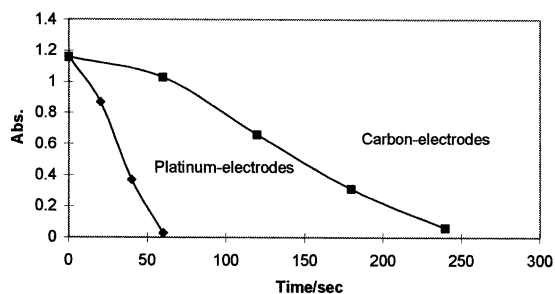


Fig. 5 Comparison of carbon and platinum electrodes ($[\text{NaCl}] = 0.2 \text{ mol/dm}^{-3}$).

Pt-electrodes. Although the decolorization rate appears at first sight to be much quicker when using platinum electrodes when compared to carbon electrodes, when the effective current densities producing these degradation rates are taken into account, ($\text{Pt} = 50 \text{ mA cm}^{-2}$; $\text{C} = 7.5 \text{ mA cm}^{-2}$), the rates of decolorization are comparable.

Effect of current density

Figure 6 shows the effect of varying the electrolysis current (50, 100, 200, and 300 mA), at constant electrolyte concentration (0.1 mol dm^{-3}), on the degradation rate of Sandolan Yellow.

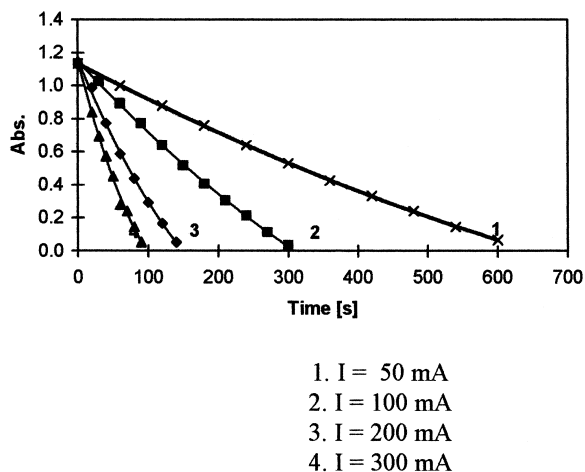


Fig. 6 Electrolysis of 50 mg dm^{-3} Sandolan Yellow: (Pt-electrodes, $[\text{NaCl}] = 0.1 \text{ mol dm}^{-3}$, $V = 500 \text{ cm}^{-3}$).

The curves fitted neither zero-order or first-order dependence. However, fitting the individual experimental curves 1–4 in Fig. 6 to a quadratic equation allowed an estimate of the initial rate of decolorization (i.e., at $t = 0$) (Table 3).

Table 3 The effect of changing current on the initial rates of degradation of Sandolan Yellow.

I/mA	0	50	100	200	300
Rate/ s^{-1}	0	0.0022	0.0046	0.0102	0.0168

These initial rates are plotted as a function of current to yield Fig. 7.

As can be seen from Fig. 7, reasonable linearity is observed, suggesting that the rate of decolorization is approximately linearly dependent on the current, i.e., doubling the current, doubles the production of hypochlorite (Faraday's law) and hence doubles the rate respectively.

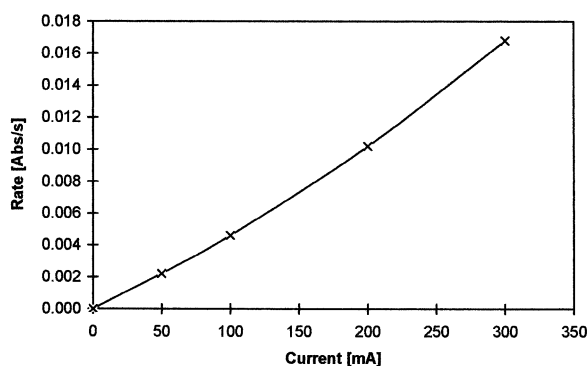


Fig. 7 Effect of current on the initial rate of degradation: (Pt-electrodes, $[\text{NaCl}] = 0.1 \text{ mol dm}^{-3}$, $V = 500 \text{ cm}^{-3}$).

Effect of changing the electrolyte concentration

Figure 8 shows the effect of changing the electrolyte concentration (0.1, 0.2, 0.3, 0.4, and 0.5 mol dm^{-3}) at constant current (100 mA) for the electrolysis of Sandolan Yellow with Pt-electrodes.

The experimental curves 1–5 (Fig. 8) were again fitted to a quadratic equation to determine the initial rate of decolorization before plotting as a function of electrolyte concentration (Fig. 9).

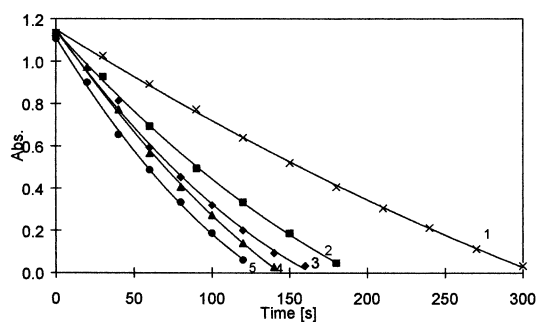


Fig. 8 Electrolysis of Sandolan Yellow at different electrolyte concentration (Pt-electrodes, $I = 100 \text{ mA}$, $V = 500 \text{ cm}^{-3}$).

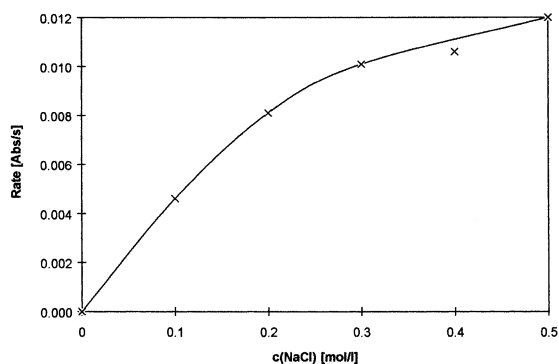
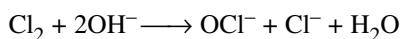
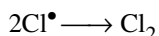
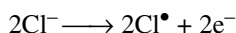


Fig. 9 Effect of electrolyte concentration ($[\text{NaCl}]/\text{mol dm}^{-3}$) on initial rate of degradation (Pt-electrodes, $I = 100 \text{ mA}$, $V = 500 \text{ cm}^{-3}$).

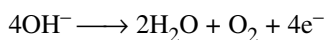
Figure 9 suggests that there is an effect of electrolyte concentration on the reaction rate. This effect is not obvious, since according to Faraday's law the amount of hypochlorite produced should have been proportional to the current and the rate should have remained constant, i.e., by applying the same current to different solutions, the same amount of hypochlorite should have been produced and the rate should have been independent (constant) of the electrolyte concentration.

One possible explanation is that the production of hypochlorite occurs in competition with the production of oxygen, e.g.,

- a. Production of hypochlorite via chlorine:



- b. Production of oxygen:



If this hypothesis is correct, then higher chloride concentrations will increase the percentage proportion of the reaction via hypochlorite and decrease the relative production of oxygen.

Effect of the type of electrolyte

Table 4 shows the effect using different electrolytes for the decolorization of a basic dye. The table shows that only chloride containing electrolytes are effective for basic dye degradation and thus points to the production of hypochlorite.

Table 4 The effect of electrolyte on the degradation of Astrazon Golden Yellow GL (7.5 mA).

Electrolyte (concentration mol dm ⁻³)	KCl (0.1)	KCl (0.05)	KCl (0.01)	KNO ₃ (0.1)	NaCl (0.1)	Na ₂ SO ₄ (0.1)
Percentage (%) dye remaining after 15 min	76	87	95	100	77	100

Effect of dye structure

Figure 10 shows the electrochemical degradation of Yoracryl Brilliant Red, Astrazon Golden Yellow GL, and Maxilon Blue GRL in the presence of potassium chloride as electrolyte (0.01 mol dm⁻³) and reinforces the observation seen during ultrasonic degradation that in general, dyes with C=C bonds are easier to degrade.

Effect of ultrasound

The purely physical effects of insonation at a solid surface suggest immediately several potential advantages of sonication as an adjunct [15] to electrochemical processing:

- Ultrasonic degassing at an electrode surface prevents gas bubble accumulation interfering with the passage of current [16].
- Agitation via cavitation at the electrode surface assists ion transport across the electrode double layer throughout the electrochemical process and reduces ion depletion in the diffusion layer.
- Cavitation at and near the electrode surface will result in continuous cleaning and activation of the electrode.

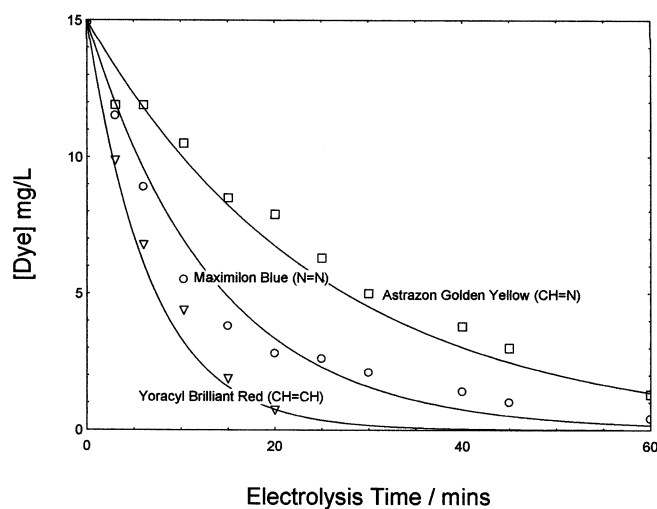


Fig. 10 Electrochemical degradation of Maximilon Blue, Astrazon Golden Yellow, and Yoracyl Brilliant red with KCl (0.01 mol dm^{-3}).

Figure 11 compares the degradation rates for the basic dye Maxilon Blue 5G using electrolysis (0.01 mol dm^{-3} KCl), sonolysis (1.1 W cm^{-2} , 510 kHz) and sonoelectrolysis (i.e., the combined sono-electrochemical treatment.)

As can be seen, at high frequency the degradation rate is accelerated in the presence of ultrasound. However, this effect appears to be reversed in the presence of low-frequency, high-power ultrasound. Figure 12 shows the results of the electrolysis of Sandolan Yellow ($[\text{NaCl}] = 0.01 \text{ mol dm}^{-3}$; $I = 60 \text{ mA}$) using two 40-kHz baths (Langford Electronics, Ltd.) of different power output (5.6 W and 29.2 W, respectively).

As can be seen in Fig. 12, the use of power ultrasound decreases the rate of decolorization with the higher intensity giving the lower rate. This can be explained by the degassing effect of ultrasound [16]. The intermediate in the reaction from chloride to hypochlorite is chlorine gas (eq. 1). If the chlo-

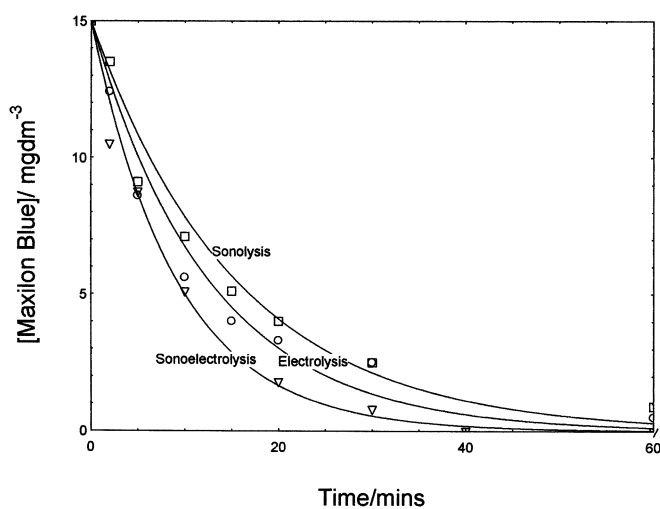


Fig. 11 Comparison of degradation techniques for Maxilon Blue 5G.

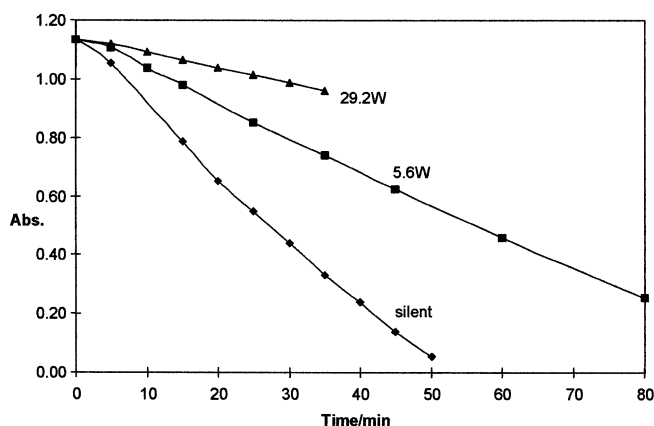


Fig. 12 The effect of irradiation power (5.6 W and 29.3 W; 40 kHz) on the electrolysis of Sandolan Yellow ($[\text{NaCl}] = 0.01 \text{ mol dm}^{-3}$; $I = 60 \text{ mA}$; Pt-electrodes).

rine can be degassed, then less hypochlorite will be produced and less decolorization will take place. In order to minimize the effect of degassing, the electrolysis was performed in a sealed cell.

Electrooxidation in a sealed cell

The sealed cell was sonicated using a probe system (Sonics & Materials, 20 kHz Vibracell) with variable power output. Initial results using very high power ultrasound led to excessive warming of the solution on prolonged sonication, making it difficult to identify whether the reduction in the rate of decrease in absorbance with time was due to reduced solubility of the chlorine or degassing—the system could not be made absolutely gas-tight. Therefore, the effect of temperature in the absence of ultrasound was investigated.

Effect of temperature in the absence of ultrasound

Solutions (Sandolan Yellow = 50 mg dm^{-3} , $[\text{NaCl}] = 0.01 \text{ mol dm}^{-3}$, $I = 60 \text{ mA}$) were electrolyzed at five different temperatures, i.e., 6.4, 12.8, 20.0, 30.0, and 40 °C. The initial rate of decolorization at each temperature was obtained using a quadratic equation as before in which the absorbance data versus time was plotted. The initial rates allowed the construction of Fig. 13.

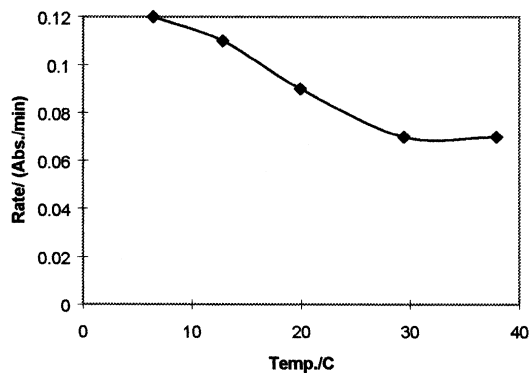


Fig. 13 Effect of temperature on rate of degradation of Sandolan Yellow ($[\text{Dye}] = 50 \text{ mg dm}^{-3}$, $[\text{NaCl}] = 0.01 \text{ mol dm}^{-3}$, $I = 60 \text{ mA}$; Pt-electrodes).

As can be seen, there is an overall reduction in the initial rate as the electrolysis temperature increases. However when these initial rates are plotted as a function of solubility, a linear relationship is obtained (Fig. 14) suggesting that in the absence of ultrasound, and at temperatures below 40 °C, the solubility of chlorine is the main parameter in determining the rate of decolorization.

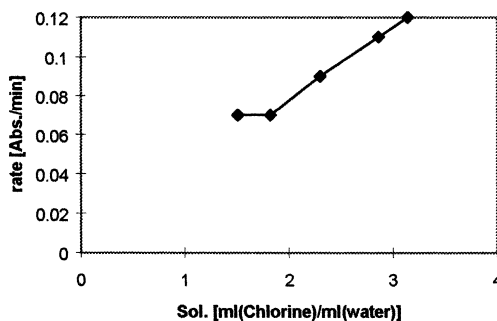


Fig. 14 Dependence of degradation rate of Sandolan Yellow on the solubility of chlorine.

Effect of ultrasonic power

Figure 15 shows the initial rates of decolorization as a function of ultrasonic intensity (16.32 W, 36.03 W, 62.79 W, 96.60 W) for the electrolysis of Sandolan Yellow (50 mg dm^{-3}) at 40.0 °C using Pt-electrodes with sodium chloride (0.01 mol dm^{-3}) as electrolyte and at 60 mA.

The figure shows that up to 30 W power input, ultrasound increases the rate by a maximum of 80%. This rate acceleration with increased power could be due to possible ultrasonic radical formation.

The rate peaks at a maximum at 30 W after which the rate decreases as the power is further increased. This phenomenon has been observed by other workers and has been explained as “damping”. If the intensity is raised above the cavitation threshold of the liquid, very “dense” cavitation zones may be created close to the probe tip, and the contact between the vibrating surface and the liquid might be lost [17,18].

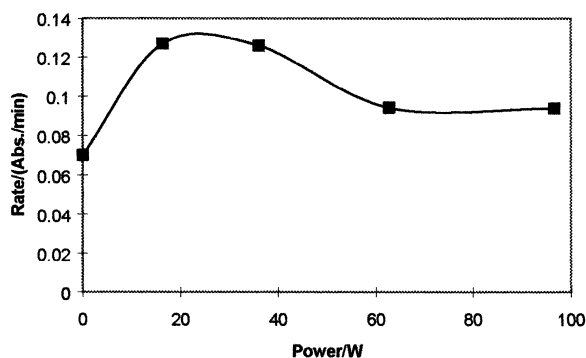


Fig. 15 Effect of ultrasonic power on the degradation rate of rate of Sandolan Yellow ($[\text{Dye}] = 50 \text{ mg dm}^{-3}$; $T = 40.0 \text{ }^\circ\text{C}$; Pt-electrodes; $[\text{NaCl}] = 0.01 \text{ mol dm}^{-3}$; $I = 60 \text{ mA}$).

CONCLUSIONS

Some of the particular advantages that accrue from the use of ultrasound in electrochemistry include [15,16]:

- a. degassing at the electrode surface
- b. disruption of the diffusion layer, which reduces depletion of electroactive species
- c. improved mass transport of ions across the diffusion layer
- d. continuous cleaning and activation of the electrode surfaces.

This paper deals with the decolorization of some basic dyes in an ultrasonic field. Since the dyes were decolorized by equivalent amounts of hydrogen peroxide, the decolorization may have been achieved by the production of OH radical (eq. 4), or the subsequent production of hydrogen peroxide (eq. 5).



This is in contrast to the decolorization of the acidic dye Sandolan Yellow, which could only be achieved by the electrolysis of the dye in aqueous sodium chloride solution; it was unaffected by ultrasound and treatment with peroxide.

The basic dyes could also be electrochemically oxidized in chloride containing media. It is argued that the liberation of chlorine at the anode results in the *in situ* generation of the powerful oxidant, hypochlorite ion.

Each electrochemical process is improved by the use of both high-frequency (low-power) and low-frequency (high-power) ultrasound. There is an optimum acoustic power when using a frequency of 20 kHz.

REFERENCES

1. M. Plattes. MSc thesis, Coventry University, UK (2000).
2. I. A. Balciogula, I. Arslan, M. T. Sacan. *Environ. Biol.* **22**, 813–822 (2001).
3. I. A. Salem and M. El-Maazawi. *Z. Phys. Chem. – Int. J. Res. in Phys. Chem. Chem. Phys.* **215**, 623–636 (2001).
4. C. Bauer, P. Jaques, A. Kalt. *J. Photochem. Photobiol. A* **140**, 87–92 (2001).
5. E. Stathatos, T. Petrova, P. Lianos. *Langmuir* **17**, 5025–5030 (2001).
6. N. H. Ince and G. Tezcanli. *Dyes Pigments* **49**, 145–153 (2001).
7. H. Destailats, A. J. Colussi, J. M. Joseph, M. R. Hoffmann. *J. Phys. Chem. A* **104**, 8930–8935 (2000).
8. N. L. Stock, J. Peller, K. Vinodgopal, P. V. Kamat. *Environ. Sci. Technol.* **34**, 1747–1750 (2000).
9. J. M. Joseph, H. Destailats, H. M. Hung, M. R. Hoffmann. *J. Phys. Chem. A* **104**, 301–307 (2000).
10. K. Vinodgopal, J. Peller, O. Makagon, P. V. Kamat. *Water Res.* **32**, 3646–3650 (1998).
11. H. Destailats, T. M. Lesko, M. Knowlton, H. Wallace, M. R. Hoffmann. *Ind. Eng. Chem. Res.* **40**, 3855–3860 (2001).
12. Y. Xiong and H. T. Karlson. *J. Environ. Sci. Health, Part A* **38**, 321–331 (2001).
13. L. Azprikowicz, C. Juzzolino, S. N. Kaul. *Water Res.* **35**, 2129–2136 (2001).
14. Z. M. Shen, W. H. Wang, J. P. Jia, J. C. Ye, X. Feng, A. Peng. *J. Hazard. Mater.* **84**, 107–116 (2001).
15. T. J. Mason, J. P. Lorimer, D. J. Walton. *Ultrasonics* **25**, 333–337 (1990).
16. F. Cataldo. *J. Electroanal. Chem.* **332**, 325–331 (1992).
17. M. A. Margulis. *Russ. J. Phys. Chem.* **48**, 1378–1380 (1974).
18. J. C. De Souza Barboza, C. Petrier, J. L. Luche. *J. Org. Chem.* **53**, 1212–1218 (1988).